BMC Musculoskeletal Disorders

BioMed Central

Research article

Open Access

Dystrophin deficiency in canine X-linked muscular dystrophy in Japan ($CXMD_J$) alters myosin heavy chain expression profiles in the diaphragm more markedly than in the tibialis cranialis muscle

Katsutoshi Yuasa*[1,2], Akinori Nakamura[2], Takao Hijikata[1] and Shinichi Takeda[2]

Address: [1]Department of Anatomy and Cell Biology, Research Institute of Pharmaceutical Sciences, Faculty of Pharmacy, Musashino University, Nishi-tokyo, Tokyo 202-8585, Japan and [2]Department of Molecular Therapy, National Institute of Neuroscience, National Center of Neurology and Psychiatry, Kodaira, Tokyo 187-8502, Japan

Email: Katsutoshi Yuasa* - k_yuasa@musashino-u.ac.jp; Akinori Nakamura - anakamu@ncnp.go.jp; Takao Hijikata - hijikata@musashino-u.ac.jp; Shinichi Takeda - takeda@ncnp.go.jp

* Corresponding author

Published: 9 January 2008

BMC Musculoskeletal Disorders 2008, **9**:1 doi:10.1186/1471-2474-9-1

Received: 28 September 2007
Accepted: 9 January 2008

This article is available from: http://www.biomedcentral.com/1471-2474/9/1

Abstract

Background: Skeletal muscles are composed of heterogeneous collections of muscle fiber types, the arrangement of which contributes to a variety of functional capabilities in many muscle types. Furthermore, skeletal muscles can adapt individual myofibers under various circumstances, such as disease and exercise, by changing fiber types. This study was performed to examine the influence of dystrophin deficiency on fiber type composition of skeletal muscles in canine X-linked muscular dystrophy in Japan ($CXMD_J$), a large animal model for Duchenne muscular dystrophy.

Methods: We used tibialis cranialis (TC) muscles and diaphragms of normal dogs and those with $CXMD_J$ at various ages from 1 month to 3 years old. For classification of fiber types, muscle sections were immunostained with antibodies against fast, slow, or developmental myosin heavy chain (MHC), and the number and size of these fibers were analyzed. In addition, MHC isoforms were detected by gel electrophoresis.

Results: In comparison with TC muscles of $CXMD_J$, the number of fibers expressing slow MHC increased markedly and the number of fibers expressing fast MHC decreased with growth in the affected diaphragm. In populations of muscle fibers expressing fast and/or slow MHC(s) but not developmental MHC of $CXMD_J$ muscles, slow MHC fibers were predominant in number and showed selective enlargement. Especially, in $CXMD_J$ diaphragms, the proportions of slow MHC fibers were significantly larger in populations of myofibers with non-expression of developmental MHC. Analyses of MHC isoforms also indicated a marked increase of type I and decrease of type IIA isoforms in the affected diaphragm at ages over 6 months. In addition, expression of developmental (embryonic and/or neonatal) MHC decreased in the $CXMD_J$ diaphragm in adults, in contrast to continuous high-level expression in affected TC muscle.

Conclusion: The $CXMD_J$ diaphragm showed marked changes in fiber type composition unlike TC muscles, suggesting that the affected diaphragm may be effectively adapted toward dystrophic stress by switching to predominantly slow fibers. Furthermore, the MHC expression profile in the $CXMD_J$ diaphragm was markedly different from that in *mdx* mice, indicating that the dystrophic dog is a more appropriate model than a murine one, to investigate the mechanisms of respiratory failure in DMD.

Background

Duchenne muscular dystrophy (DMD) is an X-linked, lethal disorder of skeletal muscle caused by mutations in the dystrophin gene, which encodes a large sub-sarcolemmal cytoskeletal protein, dystrophin. DMD is characterized by a high incidence (1 in 3,500 boys) and a high frequency of *de novo* mutation [1]. The absence of dystrophin is accompanied by the loss of dystrophin-associated glycoprotein complex from the sarcolemma, leading to reduce membrane stability of myofibers. This dysfunction results in progressive muscle weakness, cardiomyopathy, and subsequent early death by respiratory or heart failure in DMD patients.

For basic and therapeutic studies of DMD, it is very important to perform analysis and evaluation using dystrophin-deficient animal models, such as the *mdx* mouse and dystrophic dog. The *mdx* mouse has been well utilized in many DMD studies, but the murine model shows moderate dystrophic changes unlike severe human DMD [2]. In contrast, golden retriever muscular dystrophy (GRMD) shows similar dystrophic phenotypes to those of human patients: elevated serum CK level, gross muscle atrophy with joint contracture, cardiomyopathy, prominent muscle necrosis, degeneration with mineralization and concurrent regeneration, and endomysial and perimysial fibrosis [3]. Therefore, the dystrophic dog is more suitable than the *mdx* mouse for studies to gain insight into the pathogenic and molecular biological mechanisms of human DMD, as well as for pre-clinical trials [4]. Therefore, we have recently established a colony of beagle-based canine X-linked muscular dystrophy in Japan ($CXMD_J$) [5], and have demonstrated that $CXMD_J$ also exhibited severe symptoms similar to GRMD. To date, we have utilized the littermates of the $CXMD_J$ colony for pathological [6,7], molecular biological [8], and therapeutic examinations [9] of DMD.

Skeletal muscles are composed of heterogeneous populations of muscle fiber types, which contribute to a variety of functional capabilities. In addition, muscle fibers can adapt to diverse situations, such as aging, exercise, and muscular diseases, by changing fiber size or fiber type composition. Therefore, it is important to analyze fiber types to evaluate the condition of skeletal muscle with disease. Fiber types can be distinguished by biochemical, metabolic, morphological, and physiological properties. One of the most informative methods for identification of fiber types is detection of myosin heavy chain (MHC) [10,11]. Myofibers express various MHC isoforms containing slow (type I), fast (types IIA, IIX, IIB), embryonic, and neonatal forms. MHC expression, however, seems to differ between animal species and muscle types. Three MHC isoforms (types I, IIA, and IIX) have been identified in limb skeletal muscles of human and dog, while the fourth isoform, MHC IIB, is abundantly present in small mammals including mouse [10,11]. In addition, expression profiles of MHCs in dystrophin-deficient muscles have been widely examined in limb skeletal muscles of DMD patients [12] and animal models, such as the *mdx* mouse [13] and GRMD [14], but it has not been fully analyzed in skeletal muscles of a canine model. Furthermore, expanded studies of the diaphragm were restricted to that of the *mdx* mouse [13,15]. Therefore, it is important to perform detailed evaluation of fiber types and fiber sizes in limb skeletal muscles and the diaphragm of $CXMD_J$ to understand adaptations toward disease by changes in fiber type composition in the skeletal muscles of human DMD.

In this study, to investigate fiber types of myofibers in dystrophin-deficient skeletal muscles of dystrophic dogs, we evaluated the expression profiles of MHCs in tibialis cranialis (TC) muscles and diaphragms of $CXMD_J$ at various ages, by immunohistochemical and electrophoretic techniques. Briefly, we detected myofibers expressing fast type, slow type, and/or developmental MHCs. In addition, the numbers of fast or slow MHC fibers and the size distribution of these myofibers were analyzed among populations of muscle fibers with or without developmental MHC. The composition of MHC isoforms was also examined in pairs of normal and affected dogs at various ages. This is the first report of evaluation of the detailed distribution of fiber types in TC muscles and diaphragms of dystrophic dogs.

Methods

Animals

Experimental dogs were wild-type and dystrophic littermates at ages from 1 month to 3 years, from the beagle-based $CXMD_J$ breeding colony at National Center of Neurology and Psychiatry (Tokyo, Japan) [5,6]. Within a few days after birth, the genotypes (wild-type, carrier, or dystrophy) of the littermates were determined by a snapback method of single-strand conformation polymorphism (SSCP) analysis [16], and the phenotypes were also confiermed by measuring serum CK level [5]. All animals were cared for and treated in accordance with the guidelines approved by Ethics Committee for Treatment of Laboratory Animals at NCNP, where three fundamental principles (replacement, reduction, and refinement) were also considered. Adult control and $CXMD_J$ dogs (10 months to 3 years) were analyzed in early experiments (three to six animals). Series consisting of a pair of a normal dog and an affected littermate at ages of 1, 2, 4, 6 months, or 1 year old were examined in subsequent experiments. TC muscles and diaphragms were removed from the dogs after necropsy, in which euthanasia was performed by exsanguination under anesthesia with isoflurane taken to prevent unnecessary pain. TC muscle was used as a

representative limb skeletal muscle, and it corresponds to the tibialis anterior muscle in mice and humans. The muscle blocks were divided into pieces and frozen immediately in isopentane pre-cooled with liquid nitrogen.

Histological and immunohistochemical analysis

Serial transverse cryosections (10 μm thick) were stained with hematoxylin and eosin (H&E), and immunostained using anti-MHC antibodies. Immunohistochemistry was performed as described previously [17]. Cryosections were incubated with the following primary antibodies: mouse monoclonal antibodies against fast type MHC (NCL-MHCf; Novocastra), slow type MHC (NCL-MHCs), and developmental MHC (NCL-MHCd). The primary antibodies were detected using a Vectastain® ABC kit (Vector Laboratories) and then visualized with diaminobenzidine. Images were recorded using a microscope (Eclipse E600; Nikon) equipped with a CCD camera (HV-D28S; Hitachi), and fiber types of individual myofibers from 400 to 1200 per muscle were identified, based on serial sections immunostained with three types of MHC antibodies. Subsequently, the fiber number of each group was counted, and fiber sizes were also measured using Image-Pro Plus (Media Cybernetics). Furthermore, the differences in MHC expression between two groups (normal, dMHC (-) *vs* affected, dMHC (-); affected, dMHC (-) *vs* affected, dMHC (+)), between muscles (TC muscle *vs* diaphragm), or among ages (1, 2, 4, 6 months, and 1 year) were evaluated by Yates's chi-square test.

Myosin extraction and gel separation

Myosin was extracted on ice for 60 min from cryosections, as described previously [18,19]. MHC isoforms were separated on 8% SDS-polyacrylamide gels containing 30% glycerol, according to the methods described previously [19,20] with some modifications. Briefly, aliquots of 0.4 μg of total protein were loaded in each well of mini-gels (Bio-Rad). Electrophoresis was carried out at 60 V at 5°C for 48 h using upper buffer containing additional 10 mM 2-mercaptoethanol. The gels were stained with silver, and the image was scanned and analyzed using NIH image.

Results

MHC expression in TC muscle and diaphragm of adult CXMD$_J$

To investigate the relationship between the pathology and fiber types in dystrophic skeletal muscles of CXMD$_J$, we first examined histological features and MHC expression in TC muscles and diaphragms of normal and affected dogs at adult stages (10 months to 3 years old) (Fig. 1). In H&E-stained sections, affected muscles exhibited some dystrophic characteristics, such as necrosis, regeneration, cellular infiltration, fibrosis, fiber splitting, and fiber size variation. Especially, clusters of infiltrating cells were prominently observed in TC muscles, while endomysial fibrosis was predominant in diaphragms.

We next detected expression of fast and slow type MHCs for fiber type identification, and further examined developmental MHC, which means neonatal and/or embryonic MHC, as a marker of regenerating fibers (Fig. 1). In TC muscles and diaphragms of adult normal dogs, individual myofibers showed expression of either fast or slow type MHC. In affected TC muscles, the proportions of fast or slow MHC fibers were similar between normal and affected muscles. In addition, large numbers of developmental MHC-expressing fibers were observed in clusters, and many of these fibers co-expressed fast type MHC. In the affected diaphragms, the numbers of fast MHC fibers were much lower than in the normal counterparts, and slow type MHC was expressed in almost all fibers. Furthermore, the numbers of developmental MHC fibers were less than in affected TC muscle, and almost all of these fibers co-expressed slow type MHC, unlike TC muscle. These results indicated that the influences of dystrophin deficiency on MHC expression are significantly different between TC muscle and the diaphragm of CXMD$_J$, suggesting that the diaphragm would be more greatly influenced with regard to the composition of fiber types and muscle regeneration than TC muscle.

MHC expression and fiber size distribution

To further evaluate the size distribution of individual myofibers related to MHC expression, we measured transverse areas of all muscle fibers within one area in TC muscle or diaphragm of adult CXMD$_J$ (Fig. 2 and Table 1). We then analyzed three types of MHC-positive fibers (fast, slow, and hybrid) among populations of myofibers expressing fast and/or slow type MHC(s) together with or without developmental MHC, which were defined as regenerating or non-regenerating fibers, respectively. In non-regenerating fibers of affected TC muscle and diaphragm, the proportion of slow MHC fibers increased and these fibers showed a larger size distribution than those in the normal counterparts, indicating increased number and enlarged fiber size of slow fibers (Fig. 2B and Table 1). Interestingly, fast MHC fibers disappeared in the adult CXMD$_J$ diaphragm.

In regenerating fibers of both affected muscles, the distributions of all three populations shifted to smaller sizes than those in the normal counterparts, and a large number of hybrid fibers co-expressing fast and slow type MHCs were observed at a high rate (Fig. 2C and Table 1). In addition, fast MHC fibers were predominant in a regenerating population in TC muscle, while slow MHC fibers were predominant in the diaphragm except for hybrid fibers. These observations suggested that fast fibers could be more susceptible to dystrophic stress than slow fibers, and

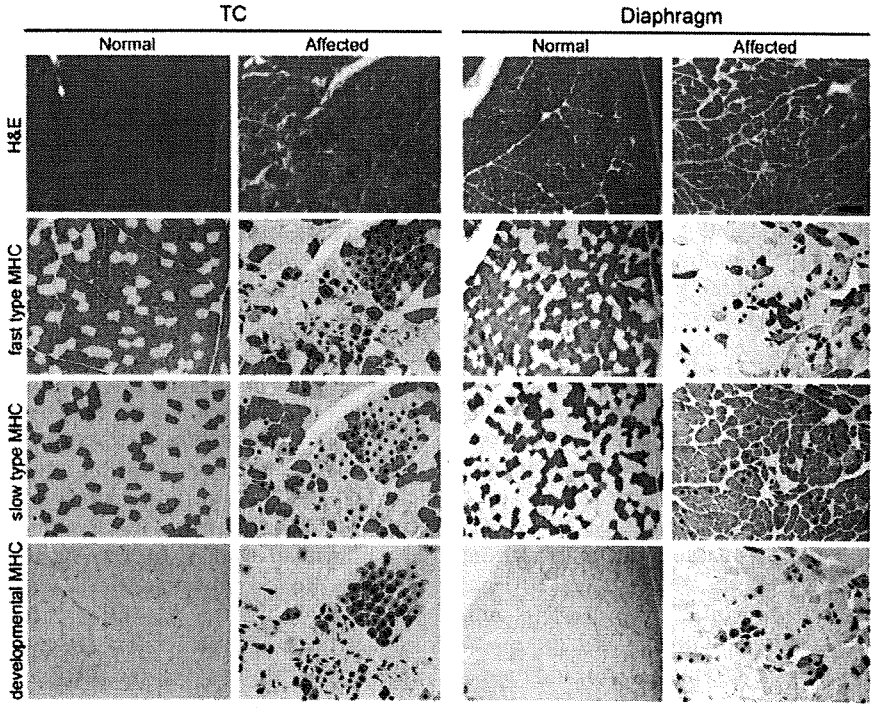

Figure 1
Representative images of histology (H&E) and expression of fast type, slow type, or developmental myosin heavy chain (MHC) in tibialis cranialis (TC) muscle and diaphragm of a normal (10 months old) or a CXMD$_J$ dog (11 months old). Identical parts of serial cross-sections are shown in longitudinal panels. In panels of affected muscles, dots show the fibers expressing developmental MHC. Bar: 200 μm.

alteration of MHC expression and regeneration of muscle fibers would be different between TC muscle and the diaphragm.

Time courses of histology and MHC expression

To investigate how MHC expression alters together with growth of CXMD$_J$, we examined MHC expression in TC muscles and diaphragms of a normal or an affected littermate at various ages from neonatal to adult stages (1 month to 1 year old) in relation to histopathological features. Affected TC muscles showed mild lesions at 1 and 2 months old, but severe degenerative lesions were evident at over 4 months old (Fig. 3). Expression of fast or slow type MHC did not alter much with aging, and developmental MHC was expressed continuously (Fig. 4). In contrast, degenerative lesions were severe in the affected diaphragm at all ages examined (from 1 month old onward), and endomysial fibrosis was dominantly present over 6 months old (Fig. 3). Fast MHC fiber number decreased markedly, while the number of slow MHC fibers increased significantly in affected diaphragms after 6 months old (Fig. 5). In addition, expression of developmental MHC decreased at 6 months and 1 year old. These observations indicated that MHC expression is altered greatly in the affected diaphragms after 6 months old, unlike TC muscles.

For quantitative evaluation of MHC expression in individual myofibers, we counted three types of MHC-expressing fibers among non-regenerating or regenerating populations within an area in the TC muscle or diaphragm of a normal or an affected littermate (Fig. 6). As normal muscles still expressed developmental MHC at 1 month old (Fig. 4 and 5), we performed the examinations at both adolescent (2 and 4 months old) and adult stages (10 or 11 months old). In normal dogs, the number of fast MHC fibers in TC muscle was three times greater than that of slow MHC fibers throughout aging, while the proportions in the diaphragms remained constant and equivalent between the two types (Fig. 6A). In non-regenerating fibers, the proportions of fiber types were not constant in affected TC muscles at the ages examined, but the majority of these fibers consisted of slow MHC fibers in the affected diaphragms (Fig. 6B). These observations indicated that slow fibers were already predominant in non-regenerating populations of CXMDJ diaphragms at younger ages. In

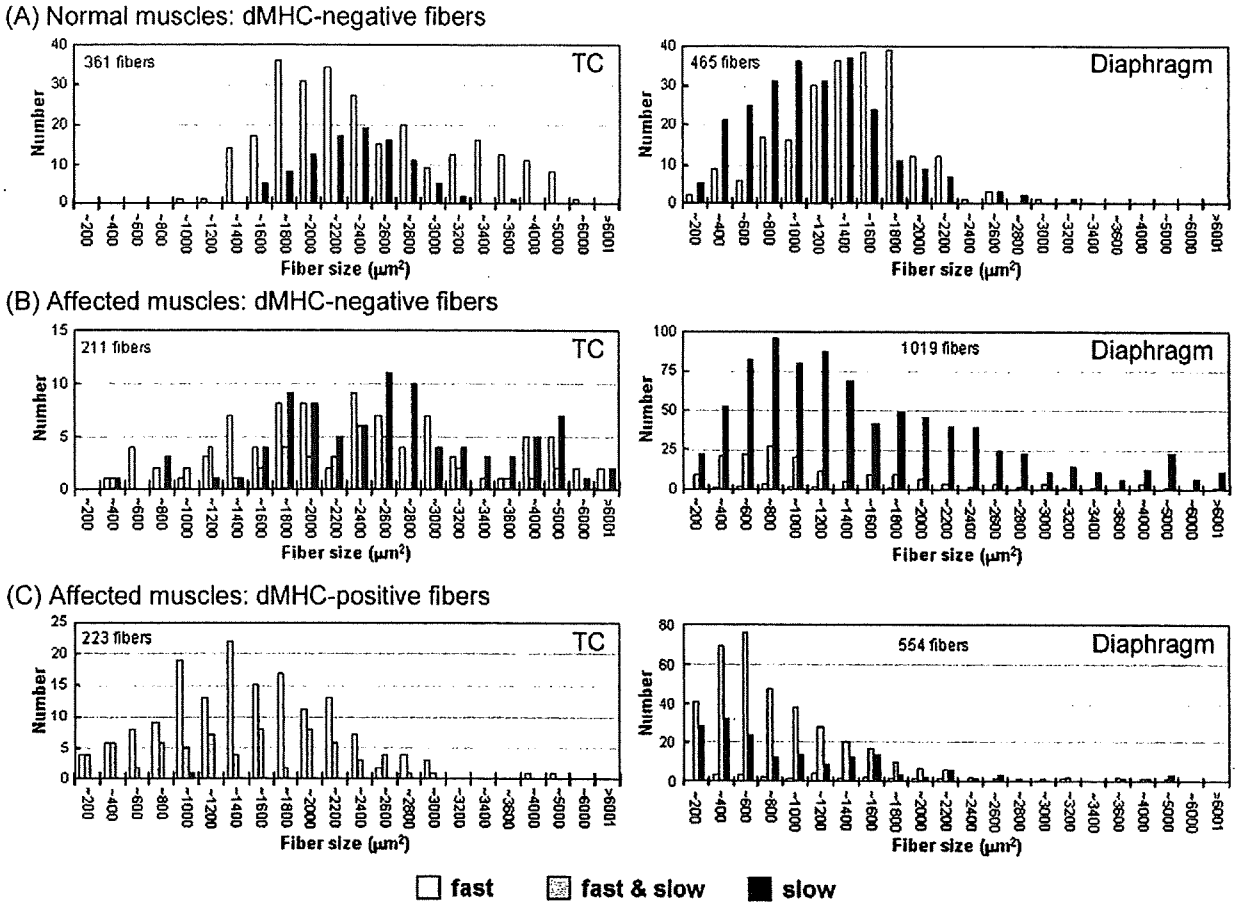

Figure 2

The size distribution of myofibers expressing fast and/or slow type MHCs in skeletal muscles of a normal (10 months old) or a CXMD$_J$ dog (11 months old). On the basis of expression of fast and slow type MHCs, all fibers within an area of TC muscle or diaphragm of a normal (A) or an affected dog (B, C) were classified into three types of MHC-positive fiber. Furthermore, fast (white), hybrid (gray), or slow MHC myofibers (black) were analyzed among populations of muscle fibers with non-expression of developmental MHC (A, B) or with expression of developmental MHC (C) in terms of fiber numbers (see Table 1) and fiber sizes (A-C). Note that larger sizes of slow MHC fibers were noticeable in populations of muscle fibers expressing fast and/or slow MHC(s) but not developmental MHC of affected muscles (B).

regenerating fibers, in contrast to the observation that fast MHC fibers consistently accounted for the majority of fibers in affected TC muscles, the affected diaphragms were mainly composed of hybrid and slow MHC fibers and the proportion increased gradually with age (Fig. 6C). These observations indicated that MHC expression in regenerating fibers was also different between affected TC muscle and diaphragm after 4 months old, although it was relatively similar in the two at 2 months old.

Temporal changes of MHC isoforms

To examine how progressive degeneration alters the composition of fiber types in affected skeletal muscles, we detected myosin isoforms in TC muscles and diaphragms of CXMD$_J$ at various ages by electrophoretic gel separation (Fig. 7). Four MHC isoforms (I, IIA, IIX, and embryonic), which migrated on electrophoresis as IIA-embryonic-IIX-I from slowest to fastest [11,12], were detected in canine skeletal muscles (Fig. 7A). In affected TC muscles, type I, IIA, and embryonic isoforms were consistently detected at similar levels, but the level of type IIX MHC was lower than those in normal TC muscles after 2 months old. In contrast, type IIA MHC level decreased gradually in affected diaphragms with growth, and type I accounted for the majority of MHC components in animals over 6 months old. In addition, the embryonic isoform

Table 1: The numbers of myofibers co-expressing fast type, slow type, and/or developmental MHCs in skeletal muscles of a normal (10 months old) or a CXMD$_J$ dog (11 months old).

	TC			Diaphragm		
	Normal	Affected		Normal	Affected	
Developmental	-	-	+	-	-	+
Fast	265 (73%)	85 (40%)	155 (70%)	222 (48%)	12 (1%)	20 (3.6%)
Fast & slow	0 (0%)	38 (18%)	67 (30%)	0 (0%)	160 (16%)	370 (66.8%)
Slow	96 (27%)	88 (42%)	1 (0%)	243 (52%)	847 (83%)	164 (29.6%)
Total	361 (100%)	211 (49%)	223 (51%)	465 (100%)	1019 (65%)	554 (35%)

The numbers of fibers analyzed were results from a normal or an affected dog. MHC expression between two groups (normal, dMHC (-) vs affected, dMHC (-); affected, dMHC (-) vs affected, dMHC (+)), or between muscles (TC muscle vs diaphragm) was analyzed by Yates's chi-square test. Significant differences ($p < 0.05$) were detected in all tests.

decreased in affected diaphragms after 6 months old. These results were consistent with those of immunohistochemical analyses (Figs. 4 and 5). These observations suggested that type IIX and IIA fast fibers may be preferentially affected in TC muscle and diaphragm of CXMD$_J$, respectively. Furthermore, these observations suggested that muscle regeneration may deteriorate from relatively younger age in the affected diaphragm, unlike TC muscle.

Discussion

To investigate the alterations in fiber types in skeletal muscles of a canine DMD model, we examined MHC expression in the TC muscle and diaphragm of CXMD$_J$ at various ages. Our results indicated that the influences of dys-

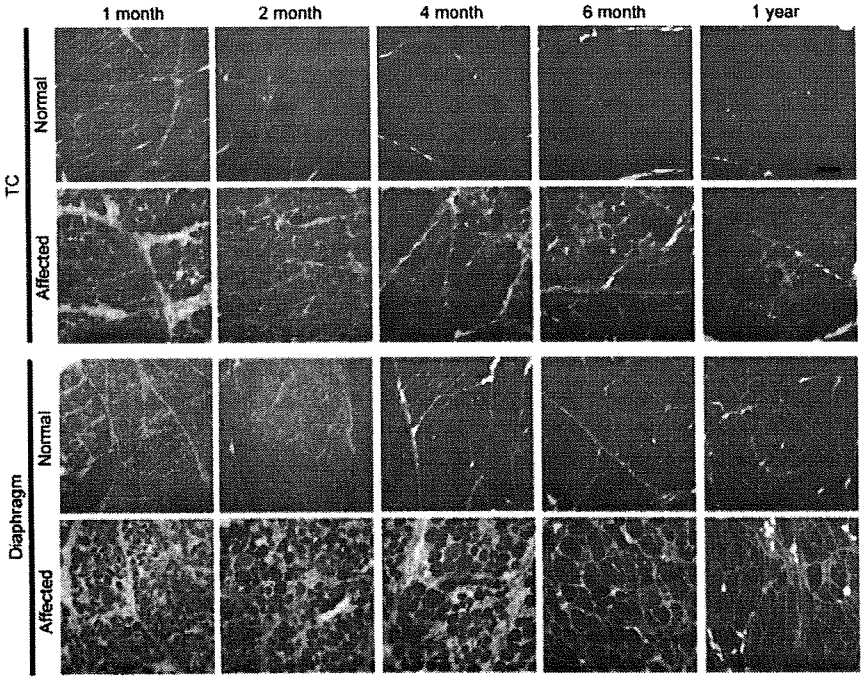

Figure 3
Representative histological findings in TC muscles and diaphragms of a normal or a CXMD$_J$ dog at 1, 2, 4, 6 months, and 1 year old. Note that severe degenerative lesions were observed from early ages in affected diaphragms, as compared with affected TC muscles. Bar: 200 μm.

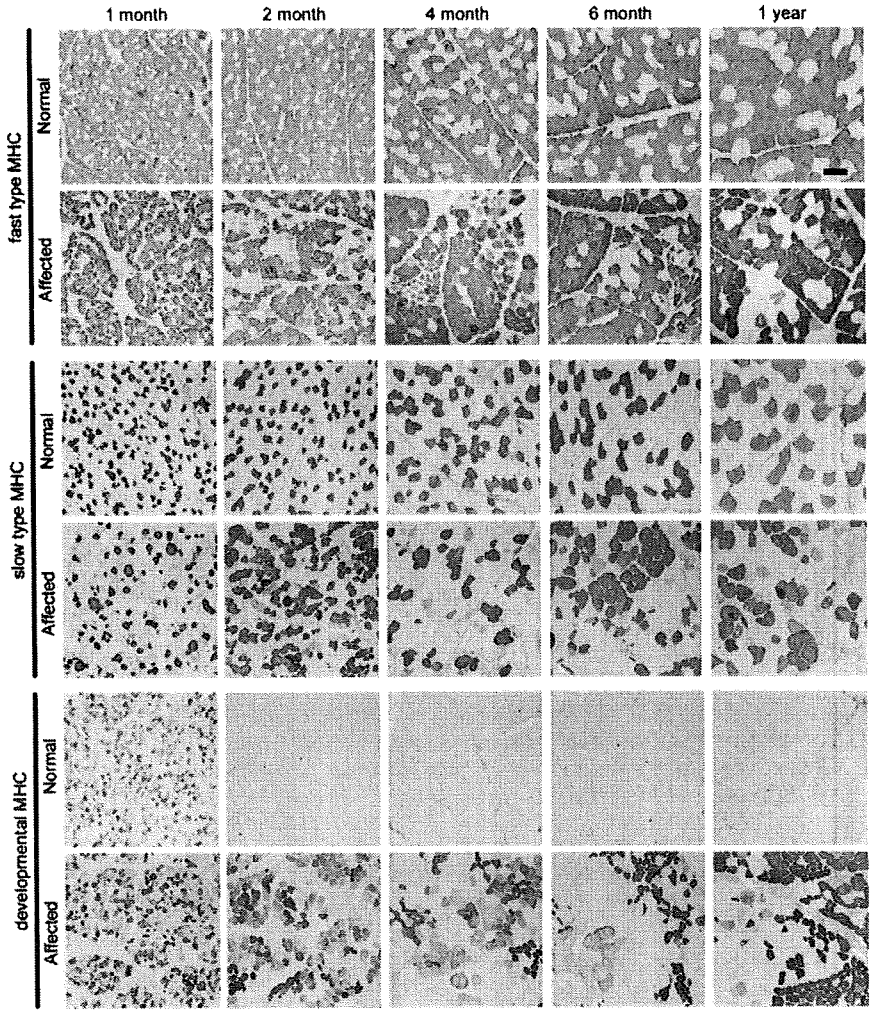

Figure 4
Expression of fast type, slow type, and developmental MHCs in TC muscles of a normal or a CXMD$_J$ dog at 1, 2, 4, 6 months, and 1 year old. Note that there were no notable differences between expression levels of fast and slow type MHCs in normal and affected TC muscles. Bar: 200 μm.

trophin deficiency on fiber type composition were significantly different between TC muscle and diaphragm.

To analyze MHC expression in details, we compared fiber type composition and fiber size distribution of MHC-expressing fibers between a normal dog (10 months old) and an affected dog (11 months old). In normal and affected dogs, body weight rapidly increased to approximately 9 kg at 4 months old, and then slightly increased to approximately 14 and 11 kg at 12 months old, respectively [5]. As body weight reflects muscle weight, muscle mass and fiber size would not extremely change in 1 month after 4 months old, especially in normal dogs. In fact, in TC muscles or diaphragms of normal dogs, there were no significant differences among compositions of fiber types and MHC isoforms after 4 months old (Fig 6 and 7). In addition, we examined normal dogs at 11, 12 and 14 months old, and affected dogs at 10, 12, 13 and 15 months old. Normal muscles of adult dogs showed similar expression of fast type, slow type, or developmental MHC at all adult ages, and affected muscles also showed similar MHC expression at examined ages (data not shown). These observations implied that there would be no significant difference in MHC expression between at 10 and 11 months old, in both of normal and affected dogs.

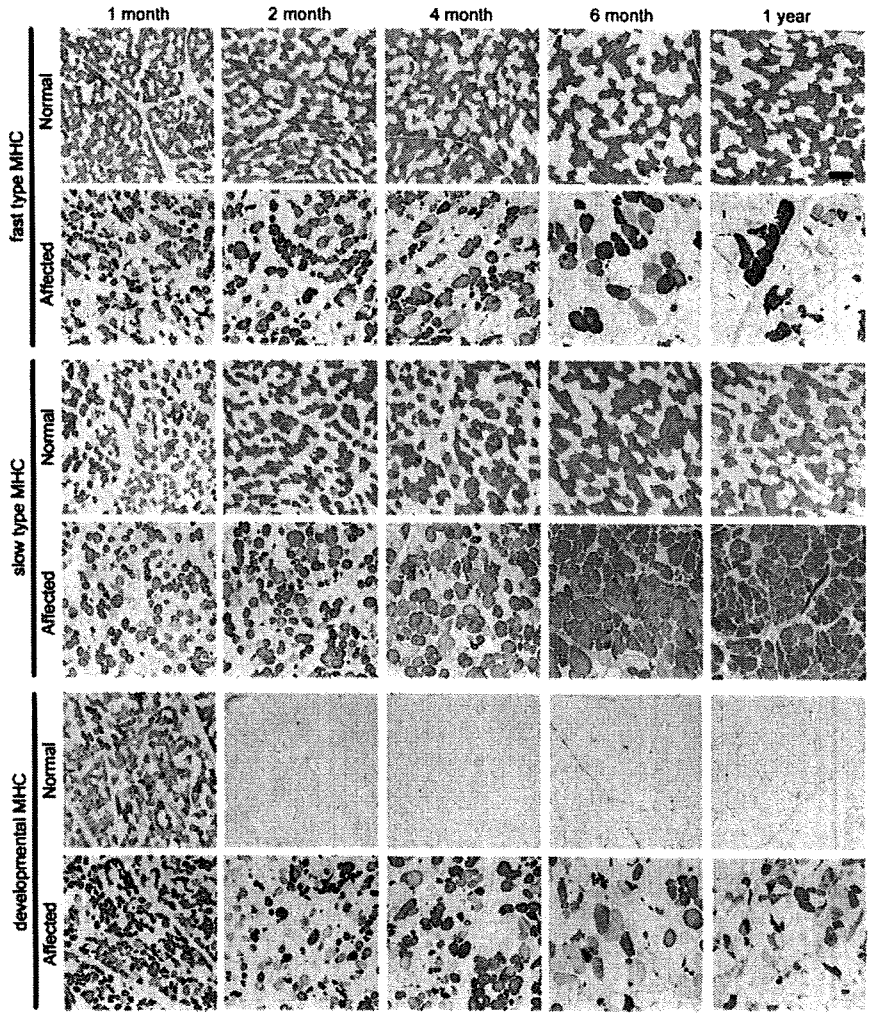

Figure 5
Expression of fast type, slow type, and developmental MHCs in diaphragms of a normal or a CXMD$_J$ dog at 1, 2, 4, 6 months, and 1 year old. Note that slow MHC fibers were increased markedly in the affected diaphragms after 6 months old, while fast MHC fibers were decreased. Bar: 200 μm.

Common features between TC muscle and diaphragm of CXMD$_J$

TC muscle and diaphragm of CXMD$_J$ shared the features that slow MHC fibers increased and enlarged selectively in non-regenerating populations, while fast type IIX or IIA MHC isoform decreased. Similar observations have been reported in skeletal muscles of the *mdx* mouse [13], GRMD [14], and human DMD [12,21]. In general, increasing and enlarging of slow fibers may be a consequence of adaptive responses by metabolic enzyme systems and energy consumption, because slow fibers have lower capacity for power output and consume less energy than fast fibers [22]. Our results also supported the hypothesis that slow fibers would be more adaptable to dystrophic stress than fast fibers, to compensate for the reduced abilities of muscle function.

Two mechanisms were considered to explain the selective increase in slow fibers during progressive muscle degeneration. One possibility is that slow fibers may be more resistant to dystrophic stress than fast fibers, leading to selective survival of slow fibers. This was supported by the observation that slower muscle fibers contained significantly more utrophin, a homolog of dystrophin, in comparison to faster counterparts [23,24]. Another is transition of MHC isoforms, where type IIA or IIX MHC

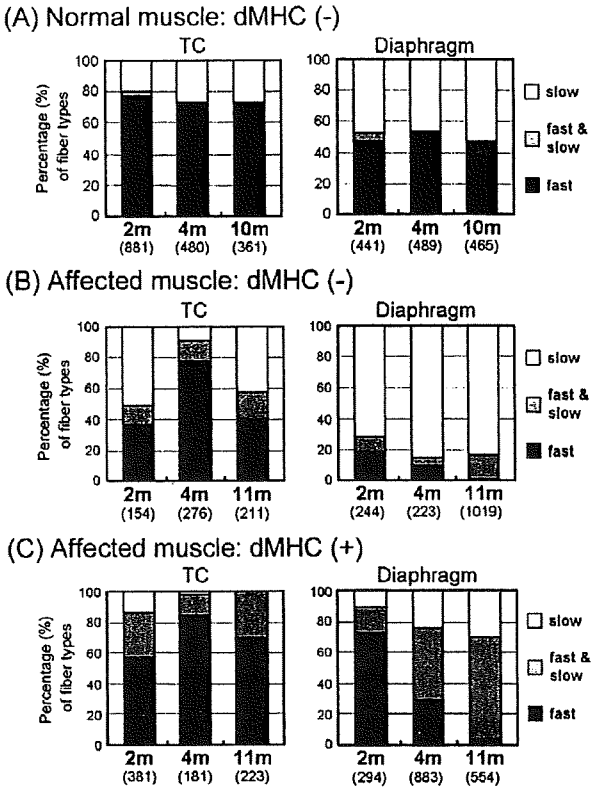

Figure 6

Proportions of fiber types in skeletal muscles of a normal or a CXMD$_J$ dog at various ages. The numbers of fast (black), hybrid (gray), and slow MHC myofibers (white) among populations of myofibers without developmental MHC (A, B) and with developmental MHC (C) were counted in TC muscle and diaphragm of a normal (A) or an affected dog (B, C) at adolescent (2 or 4 months old) or adult stages (10 or 11 months old). The numbers under the ages show total fibers examined. MHC expression between two groups (normal, dMHC (-) *vs* affected, dMHC (-); affected, dMHC (-) *vs* affected, dMHC (+)), between muscles (TC muscle *vs* diaphragm), or among ages (2, 4, and 10 or 11 months) was analyzed by Yates's chi-square test. Significant differences ($p < 0.05$) were detected in all tests, except for no significant differences between 4 and 10 months old in normal TC muscles or diaphragms. Note that slow MHC fibers were consistently larger than other fibers, in populations of muscle fibers without developmental MHC of affected diaphragms. In populations of muscle fibers co-expressing developmental MHC and other MHC isoform(s), slow MHC and hybrid fibers were increased markedly in the affected diaphragm at 4 and 11 months old, unlike TC muscles.

isoforms could be transited to type I, as seen in hypertrophy and exercise [25]. MHC I, IIa, IIx, and IIb gene expression are known to be regulated by the calcineurin pathway [26,27]. Dystrophin deficiency may accelerate MHC transition to slower types *via* calcineurin/NFAT signaling in skeletal muscles of CXMD$_J$, because calcineurin and activated NFATc1 protein content were higher in muscles from *mdx* than wild-type mice [28]. However, it remains possible that both mechanisms may be active at the same time, because the calcineurin/NFAT cascade can regulate not only the MHC promoters but also the utrophin A promoter [24,29,30].

Differences between TC muscle and diaphragm of CXMD$_J$

The CXMD$_J$ diaphragm developed severe degenerative lesions from earlier stages than TC muscle, which corresponded to previous reports [3,5,31]. In addition, dystrophic changes in the CXMD$_J$ diaphragm not only markedly altered the expression of fast and slow type MHCs but also decreased the amount of the developmental (embryonic and/or neonatal) MHC with growth, unlike affected TC muscle. Especially, fast MHC fibers disappeared and slow MHC fibers enlarged in the adult CXMD$_J$ diaphragm. The greater cross-sectional area of slow fibers in affected diaphragms might be due to hypertrophy in compensation for loss of fast fibers, relating to plasticity of muscle fibers, as mentioned above. The diaphragm keeps continuous contraction of muscle fibers without resting, while limb skeletal muscle regularly rests its movement. Therefore, replacement with slow fibers may be particularly enhanced in the diaphragm rather than TC muscle, depending on pathological severity and contractile activity of skeletal muscles.

Fiber type determination and fiber type-specific gene expression are regulated by multiple signaling pathways and transcription factors. As partially described above, a key mediator, calcineurin, plays an important role in acquisition of fiber phenotype [29,30] and may induce not only transition of MHC isoforms from faster to slower types but also transformation of myofiber phenotypes in mouse or rat muscles [26,27,32]. In addition, calcineurin signaling activity was greater in the diaphragm than in the tibialis anterior muscle of the *mdx* mouse [28]. Therefore, replacement with slow fibers may be up-regulated to a greater extent in the diaphragm than in the TC muscle of CXMD$_J$.

We also showed age-related changes of MHC expression in affected diaphragms after 6 months old, in contrast to TC muscles (Fig 4, 5 and 7). In addition, fiber type compositions in non-regenerating or regenerating fibers were also different between the TC muscle and the diaphragm, depending on age. In non-regenerating fibers of affected TC muscles, fast MHC fibers at 4 months old was higher than those at 2 and 11 months old (Fig. 6B). It might be partially involved in pathological changes that degenerative lesions appeared obviously in affected TC muscles after 4 months old, as described previously [3,5,31]. In

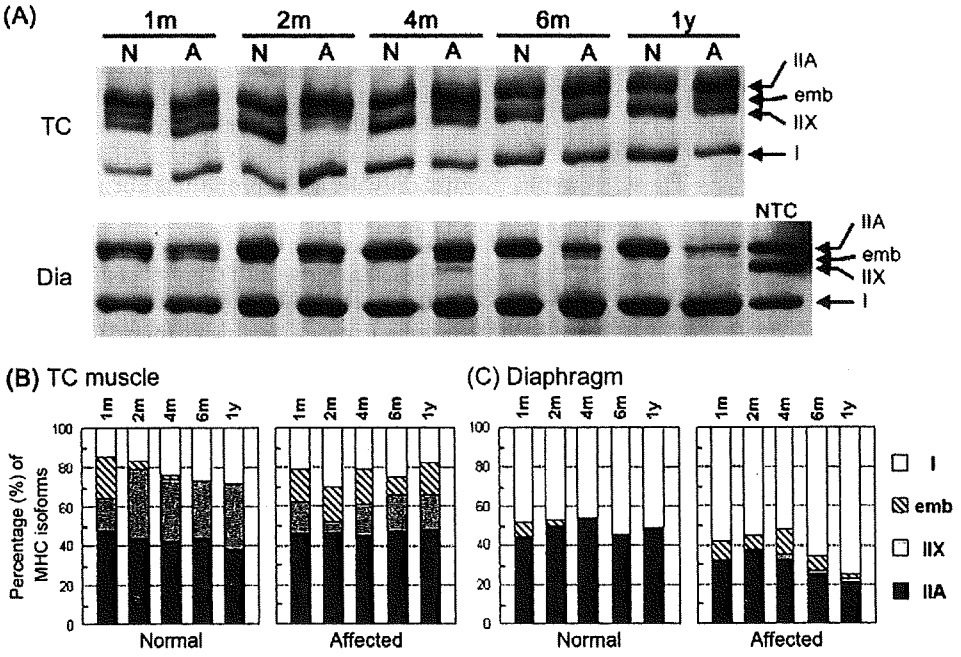

Figure 7
MHC isoforms in skeletal muscles of normal and CXMD$_J$ dogs. (A) Electrophoretic separation of MHC isoforms in TC muscle and diaphragm. Myosin was extracted from muscles at various ages (1, 2, 4, 6 months, and 1 year old), and aliquots of 0.4 μg of protein were separated on 8% SDS-polyacrylamide gels containing 30% glycerol. Four MHC isoforms (I, IIX, IIA, and embryonic) were detected. NTC: normal TC muscle at 1 year old. Note that MHC type I increased in the affected diaphragm after 6 months old. (B) Quantitative analysis of MHC isoforms. MHC expression between two groups (normal *vs* affected) or among ages (1, 2, 4, 6 months and 1 year) was analyzed by Yates's chi-square test. Significant differences ($p < 0.05$) were detected between normal and affected groups in TC muscles after 2 months old or in diaphragms after 4 months old, and between 1 and 2 months old in normal TC muscles.

regenerating fibers of the CXMD$_J$ diaphragm, the proportion of myofibers expressing slow type MHC increased markedly after 4 months old (Fig. 6C). These results suggested that MHC expression in TC muscle and the diaphragm of CXMD$_J$ would be influenced by different mechanisms after 4 months old. These age-dependent MHC expression might be related to body growth, particularly increasing of muscle mass. One possibility is participation of insulin-like growth factor (IGF)-1, which is important for postnatal growth of skeletal muscles [33] and can activate multiple Ca^{2+}-dependent signaling pathways, including the calcineurin/NFAT pathway [30]. When growth rate of body weight decreases after 4 months old [5], signaling activity of IGF-1 might reduce and MHC expression might be regulated predominantly by alternative signaling pathways.

Comparison among* mdx, *CXMD$_J$* *and DMD diaphragms

MHC expression in normal skeletal muscle has been well studied in mice [15,34], dogs [11], and humans [35]. In normal dogs, the proportions of fiber types in TC muscle were relatively similar to those in the representative tibialis anterior muscles of mice and humans. In the diaphragm, however, the proportion of fiber types differed markedly among these species. The murine diaphragm is composed mainly of fast type IIA and IIX isoforms [15,34], but the canine diaphragm consists of equal populations of slow type MHC I and fast type MHC IIA [11], as also shown in our study. In normal human diaphragm, the distribution of myosin isoforms has been estimated that types I, IIA, and IIX account for approximately 45%, 40%, and 15%, respectively [35]. Thus, the proportions of MHC isoforms in the diaphragm of healthy dogs are much closer to those of humans than those of mice.

Some groups have studied expression profiles of MHC isoforms in the diaphragm of the *mdx* mouse. The *mdx* diaphragm shows increases in MHC type I fibers and elimination of type IIX population at 2 years old, but not at young ages (3 to 6 months old) [13,15,34]. In contrast to the *mdx* diaphragm, that in CXMD$_J$ exhibited drastic changes even in younger animals (6 months old). On the

other hand, there is no direct information available regarding the changes in fiber type composition in the diaphragm in human DMD. In addition, there is an important difference of MHC expression even in limb skeletal muscles between large mammals (including dogs and humans) and mammals with smaller body mass, especially rodents. The former do not express the fastest MHC IIB isoform in limb muscles [10,11,36], while it is abundantly expressed in the latter [34]. Therefore, changes/adaptations in skeletal muscles of dogs with muscular dystrophy are likely to be more relevant to human DMD, than that in the *mdx* mouse. As it is difficult to examine the diaphragms of DMD patients, it would be important to investigate the differences between murine and canine models for understanding the mechanisms of respiratory failure in human DMD.

Conclusion

Based on fiber type classification using MHC expression, we demonstrated the predominant replacement with slow fibers and reduced muscle regeneration with progression of muscular dystrophy in the diaphragm of a canine DMD model, but these phenomena were much less strict in affected TC muscle. In addition, the expression profiles of MHC isoforms in the $CXMD_J$ diaphragm were evidently different from those of the *mdx* mouse. Our results indicated that dystrophic dog is a more appropriate model than a murine one for human DMD, and would be useful for investigation of the mechanisms of respiratory failure in DMD, as well as pathological and molecular biological backgrounds, and therapeutic effects in clinical trials.

Competing interests

The author(s) declare that they have no competing interests.

Authors' contributions

KY designed the study, carried out the pathological and immunohistological examinations, and drafted the manuscript. AN participated in interpretation of data, and helped to draft the manuscript. TH participated in coordination of the study. ST participated in the design, planning, and coordination of the study, and helped to draft the manuscript. All authors read and approved the final manuscript.

Acknowledgements

We are grateful to Dr. Madoka Yoshimura, Dr. Nobuyuki Urasawa, Dr. Naoko Yugeta, Ms. Ryoko Nakagawa, and Dr. Masayuki Tomohiro for technical assistance. We also thank Mr. Hideki Kita and Mr. Shinichi Ichikawa for care and management of experimental animals. This work was supported by Grants-in-Aid for Center of Excellence (COE), Research on Nervous and Mental Disorders (13B-1, 16B-2, 17A-10, 19A-7), Health Science Research Grants for Research on Psychiatry and Neurological Disease and Mental Health (H12-kokoro-025, H15-kokoro-021, H18-kokoro-019), and the Human Genome and Gene Therapy (H13-genome-001, H16-genome-003) from the Ministry of Health, Labor, and Welfare of Japan, and Grants-in-Aid for Scientific Research to KY and High-Tech Research Center Project for Private Universities (matching fund subsidy, 2004-2008) from the Ministry of Education, Culture, Sports, Science, and Technology of Japan.

References

1. Emery AEH: *Duchenne Muscular Dystrophy* 2nd edition. Oxford: Oxford University Press; 1993.
2. Nonaka I: **Animal models of muscular dystrophies.** *Lab Anim Sci* 1998, **48**:8-17.
3. Valentine BA, Cooper BJ, Cummings JF, De Lahunta A: **Canine X-linked muscular dystrophy: morphologic lesions.** *J Neurol Sci* 1990, **97**:1-23.
4. Howell JM, Fletcher S, Kakulas BA, O'Hara M, Lochmuller H, Karpati G: **Use of the dog model for Duchenne muscular dystrophy in gene therapy trials.** *Neuromuscul Disord* 1997, **7**:325-328.
5. Shimatsu Y, Yoshimura M, Yuasa K, Urasawa N, Tomohiro M, Nakura M, Tanigawa M, Nakamura A, Takeda S: **Major clinical and histopathological characteristics of canine X-linked muscular dystrophy in Japan, CXMDJ.** *Acta Myol* 2005, **24**:145-154.
6. Shimatsu Y, Katagiri K, Furuta T, Nakura M, Tanioka Y, Yuasa K, Tomohiro M, Kornegay JN, Nonaka I, Takeda S: **Canine X-linked muscular dystrophy in Japan (CXMDJ).** *Exp Anim* 2003, **52**:93-97.
7. Yugeta N, Urasawa N, Fujii Y, Yoshimura M, Yuasa K, Wada MR, Nakura M, Shimatsu Y, Tomohiro M, Takahashi A, Machida N, Wakao Y, Nakamura A, Takeda S: **Cardiac involvement in Beagle-based canine X-linked muscular dystrophy in Japan (CXMDJ): electrocardiographic, echocardiographic, and morphologic studies.** *BMC Cardiovasc Disord* 2006, **6**:47.
8. Fukushima K, Nakamura A, Ueda H, Yuasa K, Yoshida K, Takeda S, Ikeda S: **Activation and localization of matrix metalloproteinase-2 and -9 in the skeletal muscle of the muscular dystrophy dog (CXMDJ).** *BMC Musculoskelet Disord* 2007, **8**:54.
9. Yuasa K, Yoshimura M, Urasawa N, Ohshima S, Howell JM, Nakamura A, Hijikata T, Miyagoe-Suzuki Y, Takeda S: **Injection of a recombinant AAV serotype 2 into canine skeletal muscles evokes strong immune responses against transgene products.** *Gene Ther* 2007, **14**:1249-1260.
10. Scott W, Stevens J, Binder-Macleod SA: **Human skeletal muscle fiber type classifications.** *Phys Ther* 2001, **81**:1810-1816.
11. Toniolo L, Maccatrozzo L, Patruno M, Pavan E, Caliaro F, Rossi R, Rinaldi C, Canepari M, Reggiani C, Mascarello F: **Fiber types in canine muscles: myosin isoform expression and functional characterization.** *Am J Physiol Cell Physiol* 2007, **292**:C1915-1926.
12. Marini JF, Pons F, Leger J, Loffreda N, Anoal M, Chevallay M, Fardeau M, Leger JJ: **Expression of myosin heavy chain isoforms in Duchenne muscular dystrophy patients and carriers.** *Neuromuscul Disord* 1991, **1**:397-409.
13. Muller J, Vayssiere N, Royuela M, Leger ME, Muller A, Bacou F, Pons F, Hugon G, Mornet D: **Comparative evolution of muscular dystrophy in diaphragm, gastrocnemius and masseter muscles from old male *mdx* mice.** *J Muscle Res Cell Motil* 2001, **22**:133-139.
14. Lanfossi M, Cozzi F, Bugini D, Colombo S, Scarpa P, Morandi L, Galbiati S, Cornelio F, Pozza O, Mora M: **Development of muscle pathology in canine X-linked muscular dystrophy. I. Delayed postnatal maturation of affected and normal muscle as revealed by myosin isoform analysis and utrophin expression.** *Acta Neuropathol* 1999, **97**:127-138.
15. Petrof BJ, Stedman HH, Shrager JB, Eby J, Sweeney HL, Kelly AM: **Adaptations in myosin heavy chain expression and contractile function in dystrophic mouse diaphragm.** *Am J Physiol* 1993, **265**:C834-841.
16. Honeyman K, Carville KS, Howell JM, Fletcher S, Wilton SD: **Development of a snapback method of single-strand conformation polymorphism analysis for genotyping Golden Retrievers for the X-linked muscular dystrophy allele.** *Am J Vet Res* 1999, **60**:734-737.
17. Yuasa K, Sakamoto M, Miyagoe-Suzuki Y, Tanouchi A, Yamamoto H, Li J, Chamberlain JS, Xiao X, Takeda S: **Adeno-associated virus vector-mediated gene transfer into dystrophin-deficient skeletal muscles evokes enhanced immune response against the transgene product.** *Gene Ther* 2002, **9**:1576-1588.

18. Butler-Browne GS, Whalen RG: **Myosin isozyme transitions occurring during the postnatal development of the rat soleus muscle.** *Dev Biol* 1984, **102**:324-334.
19. Hosaka Y, Yokota T, Miyagoe-Suzuki Y, Yuasa K, Imamura M, Matsuda R, Ikemoto T, Kameya S, Takeda S: **Alpha1-syntrophin-deficient skeletal muscle exhibits hypertrophy and aberrant formation of neuromuscular junctions during regeneration.** *J Cell Biol* 2002, **158**:1097-1107.
20. Agbulut O, Li Z, Mouly V, Butler-Browne GS: **Analysis of skeletal and cardiac muscle from desmin knock-out and normal mice by high resolution separation of myosin heavy-chain isoforms.** *Biol Cell* 1996, **88**:131-135.
21. Webster C, Silberstein L, Hays AP, Blau HM: **Fast muscle fibers are preferentially affected in Duchenne muscular dystrophy.** *Cell* 1988, **52**:503-513.
22. Crow MT, Kushmerick MJ: **Chemical energetics of slow- and fast-twitch muscles of the mouse.** *J Gen Physiol* 1982, **79**:147-166.
23. Gramolini AO, Belanger G, Thompson JM, Chakkalakal JV, Jasmin BJ: **Increased expression of utrophin in a slow vs. a fast muscle involves posttranscriptional events.** *Am J Physiol Cell Physiol* 2001, **281**:C1300-1309.
24. Chakkalakal JV, Stocksley MA, Harrison MA, Angus LM, Deschenes-Furry J, St-Pierre S, Megeney LA, Chin ER, Michel RN, Jasmin BJ: **Expression of utrophin A mRNA correlates with the oxidative capacity of skeletal muscle fiber types and is regulated by calcineurin/NFAT signaling.** *Proc Natl Acad Sci USA* 2003, **100**:7791-7796.
25. Gregory P, Low RB, Stirewalt WS: **Changes in skeletal-muscle myosin isoenzymes with hypertrophy and exercise.** *Biochem J* 1986, **238**:55-63.
26. Dunn SE, Burns JL, Michel RN: **Calcineurin is required for skeletal muscle hypertrophy.** *J Biol Chem* 1999, **274**:21908-21912.
27. Allen DL, Sartorius CA, Sycuro LK, Leinwand LA: **Different pathways regulate expression of the skeletal myosin heavy chain genes.** *J Biol Chem* 2001, **276**:43524-43533.
28. Stupka N, Michell BJ, Kemp BE, Lynch GS: **Differential calcineurin signalling activity and regeneration efficacy in diaphragm and limb muscles of dystrophic *mdx* mice.** *Neuromuscul Disord* 2006, **16**:337-346.
29. Spangenburg EE, Booth FW: **Molecular regulation of individual skeletal muscle fiber types.** *Acta Physiol Scand* 2003, **178**:413-424.
30. Michel RN, Dunn SE, Chin ER: **Calcineurin and skeletal muscle growth.** *Proc Nutr Soc* 2004, **63**:341-349.
31. Valentine BA, Cooper BJ: **Canine X-linked muscular dystrophy: selective involvement of muscles in neonatal dogs.** *Neuromuscul Disord* 1991, **1**:31-38.
32. Chin ER, Olson EN, Richardson JA, Yang Q, Humphries C, Shelton JM, Wu H, Zhu W, Bassel-Duby R, Williams RS: **A calcineurin-dependent transcriptional pathway controls skeletal muscle fiber type.** *Genes Dev* 1998, **12**:2499-509.
33. Lupu F, Terwilliger JD, Lee K, Segre GV, Efstratiadis A: **Roles of growth hormone and insulin-like growth factor 1 in mouse postnatal growth.** *Dev Biol* 2001, **229**:141-162.
34. Coirault C, Lambert F, Marchand-Adam S, Attal P, Chemla D, Lecarpentier Y: **Myosin molecular motor dysfunction in dystrophic mouse diaphragm.** *Am J Physiol* 1999, **277**:C1170-1176.
35. Polla B, D'Antona G, Bottinelli R, Reggiani C: **Respiratory muscle fibres: specialisation and plasticity.** *Thorax* 2004, **59**:808-817.
36. Snow DH, Billeter R, Mascarello F, Carpene E, Rowlerson A, Jenny E: **No classical type IIB fibres in dog skeletal muscle.** *Histochemistry* 1982, **75**:53-65.

Pre-publication history

The pre-publication history for this paper can be accessed here:

http://www.biomedcentral.com/1471-2474/9/1/prepub

J Hum Genet (2008) 53:1012–1015
DOI 10.1007/s10038-008-0336-5

SHORT COMMUNICATION

LRRK2 P755L variant in sporadic Parkinson's disease

Hiroyuki Tomiyama · Ikuko Mizuta · Yuanzhe Li · Manabu Funayama · Hiroyo Yoshino · Lin Li · Miho Murata · Mitsutoshi Yamamoto · Shin-ichiro Kubo · Yoshikuni Mizuno · Tatsushi Toda · Nobutaka Hattori

Received: 20 June 2008 / Accepted: 31 August 2008 / Published online: 16 October 2008

Abstract Parkinson's disease (PD) is a neurodegenerative disorder of unknown etiology with probable involvement of genetic-environmental factors. The majority of PD cases (approximately 90–95%) are sporadic, while familial cases account for approximately 5–10% of PD. In a recent report, a heterozygous *LRRK2* P755L mutation within *LRRK2* exon 19 was found in 2% of Chinese sporadic PD patients and in 0% of normal controls or Caucasians, suggesting that the mutation is disease-associated with ethnic specificity. To further evaluate the role of *LRRK2* P755L variant in sporadic PD, we performed direct sequencing of *LRRK2* exon 19 in 501 Japanese sporadic PD patients (male 249, female 252, aged 28–92 years, mean 65.0 years) and 583 controls of the Japanese general population as an extended association study. In this group, we found six patients (6/501 = 1.2%) and eight controls of the general population (8/583 = 1.6%) with a heterozygous P755L variant ($P = 0.80$, $\chi^2 = 0.064$). No other variants were found in exon 19. Together with previous reports, our extended case-controlled study of large sample size suggests that *LRRK2* P755L is a non-disease-associated polymorphism in PD patients.

Keywords Parkinson's disease · Genetics · *PARK8* · *Leucine-rich repeat kinase 2 (LRRK2)* · Polymorphism · Association study · Japanese · Ethnic background

H. Tomiyama · Y. Li · L. Li · S.-i. Kubo · N. Hattori (✉)
Department of Neurology,
Juntendo University School of Medicine,
2-1-1 Hongo, Bunkyo-ku, Tokyo 113-8421, Japan
e-mail: nhattori@med.juntendo.ac.jp

I. Mizuta · T. Toda
Division of Clinical Genetics,
Osaka University Graduate School of Medicine,
Suita, Japan

I. Mizuta · M. Murata · M. Yamamoto · T. Toda · N. Hattori
Core Research for Evolutional Science and Technology (CREST), Japan Science and Technology Agency,
Saitama, Japan

M. Funayama · H. Yoshino · Y. Mizuno
Research Institute for Diseases of Old Age,
Juntendo University School of Medicine, Tokyo, Japan

M. Murata
Department of Neurology, Musashi Hospital,
National Center of Neurology and Psychiatry, Tokyo, Japan

M. Yamamoto
Department of Neurology,
Kagawa Prefectural Central Hospital, Takamatsu, Japan

Introduction

Parkinson's disease (PD, OMIM #168600) is the second most common neurodegenerative disorder next to Alzheimer's disease. The clinical features are characterized by levodopa-responsive parkinsonism, such as rigidity, resting tremor, bradykinesia, and postural instability. Although the cause of PD remains unclear, genetic-environmental interaction is suggested for the development of the disease. One of the autosomal-dominant forms of PD, *PARK8*, was originally mapped from a Japanese Sagamihara family (Funayama et al. 2002) and *LRRK2* (*PARK8*; *leucine-rich repeat kinase 2*, OMIM *609007) was identified as the causative gene for *PARK8*-linked PD (Paisán-Ruíz et al. 2004; Zimprich et al. 2004). Among *LRRK2* mutations, the most common *LRRK2* G2019S mutation in North Africans and Ashkenazi Jews has shown ethnic differences among Caucasian, Japanese, and Chinese (Nichols et al. 2005; Gilks et al. 2005; Lesage et al. 2006; Tomiyama et al.

2006; Tan et al. 2005). On the other hand, *LRRK2* G2385R variant has recently been found the most common genetic risk factor among Chinese and Japanese, but not Caucasians (Di Fonzo et al. 2006; Funayama et al. 2007; Tan et al. 2007; Farrer et al. 2007). Moreover, in a recent report (Wu et al. 2006), a heterozygous *LRRK2* p.P755L (c.2264c > *t*, rs34410987) mutation within *LRRK2* exon 19, corresponding to a predicted ankyrin-repeat-like domain of LRRK2, was found in 2% (12/598) of Chinese sporadic PD and 0% (0/765) of Chinese normal controls, suggesting its association with the disease. However, *LRRK2* P755L was reported as a polymorphism (3% of 92 normal controls) in the dbSNP database of Taiwanese. Thus, to determine the frequency and the role of *LRRK2* P755L in Asian PD, we screened for *LRRK2* exon 19 in Japanese sporadic PD patients.

Subjects and methods

The nucleotide sequences of *LRRK2* exon 19 were determined by direct sequencing in 501 sporadic Japanese PD patients and 583 controls of the Japanese general population (Table 1). All blood samples and clinical information were obtained by the attending neurologists after obtaining informed consent from their patients. The study was approved by the ethics review committees of Juntendo and Osaka Universities. Diagnosis of PD was made by the attending neurologists based on the presence of parkinsonism and good response to anti-PD treatment. Controls of the Japanese general population were evaluated by neurologists to ensure none of them had PD. DNA was prepared using standard methods. They were amplified by polymerase chain reaction (PCR) of exon 19 and sequenced using BigDye Terminator Chemistry and ABI310 and 3130 Genetic Analyzer (Applied Biosystems, Foster City, CA). Sequences of the primers, conditions of PCR, and conditions of sequencing were based on a previous report (Zimprich et al. 2004).

Results

We found 6 patients (6/501 = 1.2%) and 8 controls of the Japanese general population (8/583 = 1.6%) with a heterozygous P755L variant ($P = 0.80$, odds ratio = 1.15, 95% CI: 0.40–3.32, $\chi^2 = 0.064$) in *LRRK2* exon 19 (Table 2). No other variants were found in exon 19.

Discussion

The purpose of the present study was to clarify the role of an ethnic-specific variant in the causative gene for PD. Although PD is considered a heterogeneous disease with genetic-environmental interaction, some cases certainly exhibit a Mendelian-inherited disease or are associated with strong genetic and ethnic background. Indeed, the reported frequency of *LRRK2* G2385R was higher in Asian sporadic PD patients than in controls (Di Fonzo et al. 2006; Funayama et al. 2007; Tan et al. 2007), although this is not the case in Caucasians. Moreover, Wu et al. (2006) in Nanjing, China, recently reported that a heterozygous *LRRK2* P755L mutation was found in 2% (12/598) of Chinese sporadic PD and 0% (0/765) of normal controls, whereas none (0/463) of the Caucasian PD patients had this mutation (Deng et al. 2007), suggesting ethnic differences, like *LRRK2* G2385R. However, our results of large case-controlled study in Japanese revealed that *LRRK2* P755L is a non-disease associated polymorphism. Consistent with our data, this variant was present at similar frequency in Taiwanese PD patients (7/578 = 0.99%) and Taiwanese normal controls (10/339 = 0.97%) (Di Fonzo et al. 2006). Furthermore, the latest report in the Chinese population in Singapore showed the absence of segregation and association of P755L with PD (case 4/204 = 2.0%, control 6/235 = 2.6%, $P = 0.76$) (Tan et al. 2008). These findings might be based on ethnic or native differences in human migration history or human genetics.

We reported previously that the most common *LRRK2* G2019S mutation in Mendelian-inherited and sporadic PD

Table 1 Profile of analyzed samples in this study

Parameter	Patients	Controls of general population
Total sample, *n* (%)	501 (100)	583 (100)
Male, *n* (%)	249 (49.7)	312 (53.5)
Female, *n* (%)	252 (50.3)	271 (46.5)
Age at sampling (years)[a]	65.0 ± 9.6 (28–92)	45.0 ± 17.0 (21–98)
Male[a]	64.3 ± 10.2 (28–92)	43.6 ± 15.0 (22–92)
Female[a]	65.4 ± 9.9 (28–92)	46.8 ± 19.0 (21–98)
Age at onset (years)[a]	58.0 ± 10.5 (20–88)	
Male[a]	57.7 ± 10.9 (20–88)	
Female[a]	58.3 ± 10.1 (25–82)	

[a] Data are mean ± SD (range)

Table 2 Allele frequency of *LRRK2* c. 2264C > T (p. P755L) in Japanese patients with Parkinson's disease and controls of general population

	Genotype, *n* (%)			Allele, *n* (%)			
	C/C	C/T	T/T	C	T	χ^{2a}	OR (95% CI)
Patients (n = 501)	495 (98.8)	6 (1.2)	0 (0)	996 (99.4)	6 (0.6)	0.06	1.15 (0.40–3.32)
Controls of general population (n = 583)	575 (98.6)	8 (1.4)	0 (0)	1,158 (99.3)	8 (0.7)		

[a] Compared with the control

OR odds ratio, *CI* confidence interval

was rare in Asians compared to North Africans or Caucasians (Tomiyama et al. 2006). *LRRK2* variants are reported to spread worldwide with some ethnic differences among each variant, such as R1441G, R1441C, R1441H (exon 31, ROC domain), G2019S, I2020T (exon 41, MAPKKK domain), and G2385R (exon 48, WD40 domain) (Mata et al. 2005). Since *LRRK2* consists of as many as 51 exons, it is important to decide which exon(s) of this gene should be screened first for efficient analysis of mutation in patients with various ethnic backgrounds. In this regard, *LRRK2* exon 41 and 31 are reasonable to be screened first; however, exon 19 is not likely a candidate exon for causative mutation screening in PD. In addition, although MAPKKK and ROC domain are reported to be associated with kinase activity of LRRK2 (Paisán-Ruíz et al. 2004; Zimprich et al. 2004; Smith et al. 2006), the existence and the role of the predicted ankyrin repeat-like domain in LRRK2 have not been established yet.

So far, *LRRK2* P755L as well as G2385R variants have been found in only Chinese, Taiwanese, and Japanese (Asians) with similar frequencies in some Asians, but have not been found in Caucasians. Thus, these variants could occur independently in very ancient Asians with a single founder effect (Farrer et al. 2007). Although the HapMap project has been very successful, the presence of ethnic differences among *LRRK2* variants such as G2019S, R1441G, G2385R, and P755L suggest that further establishment of ethnic-specific or native-specific data is essential for more accurate SNP analyses and genome-wide association studies.

Conclusion

Our extended association study in Japanese with large sample size suggests that *LRRK2* P755L is a non-disease-associated polymorphism in PD patients.

Acknowledgments The authors thank all the participants. The authors also thank Ms. Yuko Nakabayashi and Ms. Yoko Imamichi for the excellent technical assistance. This work was supported by a grant from Core Research for Evolutional Science and Technology (CREST) of the Japan Science and Technology Agency (JST) and by Grants-in-Aid from the Research Committee of CNS Degenerative Diseases, the Ministry of Health, Labor, and Welfare of Japan.

References

Deng H, Le W, Huang M, Xie W, Pan T, Jankovic J (2007) Genetic analysis of LRRK2 P755L variant in Caucasian patients with Parkinson's disease. Neurosci Lett 419:104–107

Di Fonzo A, Wu-Chou YH, Lu CS, van Doeselaar M, Simons EJ, Rohé CF, Chang HC, Chen RS, Weng YH, Vanacore N, Breedveld GJ, Oostra BA, Bonifati V (2006) A common missense variant in the LRRK2 gene, Gly2385Arg, associated with Parkinson's disease risk in Taiwan. Neurogenetics 7:133–138

Farrer MJ, Stone JT, Lin CH, Dächsel JC, Hulihan MM, Haugarvoll K, Ross OA, Wu RM (2007) Lrrk2 G2385R is an ancestral risk factor for Parkinson's disease in Asia. Parkinsonism Relat Disord 13:89–92

Funayama M, Hasegawa K, Kowa H, Saito M, Tsuji S, Obata F (2002) A new locus for Parkinson's disease (PARK8) maps to chromosome 12p11.2–q13.1. Ann Neurol 51:296–301

Funayama M, Li Y, Tomiyama H, Yoshino H, Imamichi Y, Yamamoto M, Murata M, Toda T, Mizuno Y, Hattori N (2007) Leucine-rich repeat kinase 2 G2385R variant is a risk factor for Parkinson disease in Asian population. NeuroReport 18:273–275

Gilks WP, Abou-Sleiman PM, Gandhi S, Jain S, Singleton A, Lees AJ, Shaw K, Bhatia KP, Bonifati V, Quinn NP, Lynch J, Healy DG, Holton JL, Revesz T, Wood NW (2005) A common LRRK2 mutation in idiopathic Parkinson's disease. Lancet 365:415–416

Lesage S, Durr A, Tazir M, Lohmann E, Leutenegger AL, Janin S, Pollak P, Brice A, French Parkinson's Disease Genetics Study Group (2006) LRRK2 G2019S as a cause of Parkinson's disease in North African Arabs. N Engl J Med 354:422–423

Mata IF, Kachergus JM, Taylor JP, Lincoln S, Aasly J, Lynch T, Hulihan MM, Cobb SA, Wu RM, Lu CS, Lahoz C, Wszolek ZK, Farrer MJ (2005) Lrrk2 pathogenic substitutions in Parkinson's disease. Neurogenetics 17:1–7

Nichols WC, Pankratz N, Hernandez D, Paisán-Ruíz C, Jain S, Halter CA, Michaels VE, Reed T, Rudolph A, Shults CW, Singleton A, Foroud T, Parkinson Study Group-PROGENI investigators (2005) Genetic screening for a single common LRRK2 mutation in familial Parkinson's disease. Lancet 365:410–412

Paisán-Ruíz C, Jain S, Evans EW, Gilks WP, Simón J, van der Brug M, López de Munain A, Aparicio S, Gil AM, Khan N, Johnson J, Martinez JR, Nicholl D, Carrera IM, Pena AS, de Silva R, Lees A, Martí-Massó JF, Pérez-Tur J, Wood NW, Singleton AB (2004) Cloning of the gene containing mutations that cause PARK8-linked Parkinson's disease. Neuron 44:595–600

Smith WW, Pei Z, Jiang H, Dawson VL, Dawson TM, Ross CA (2006) Kinase activity of mutant LRRK2 mediates neuronal toxicity. Nat Neurosci 9(10):1231–1233

Tan EK, Shen H, Tan LC, Farrer M, Yew K, Chua E, Jamora RD, Puvan K, Puong KY, Zhao Y, Pavanni R, Wong MC, Yih Y, Skipper L, Liu JJ (2005) The G2019S LRRK2 mutation is uncommon in an Asian cohort of Parkinson's disease patients. Neurosci Lett 384:327–329

Tan EK, Zhao Y, Skipper L, Tan MG, Di Fonzo A, Sun L, Fook-Chong S, Tang S, Chua E, Yuen Y, Tan L, Pavanni R, Wong MC, Kolatkar P, Lu CS, Bonifati V, Liu JJ (2007) The LRRK2 Gly2385Arg variant is associated with Parkinson's disease: genetic and functional evidence. Hum Genet 120:857–863

Tan EK, Lim HQ, Yuen Y, Zhao Y (2008) Pathogenicity of LRRK2 P755L variant in Parkinson's disease. Mov Disord (online 8 Feb 2008)

Tomiyama H, Li Y, Funayama M, Hasegawa K, Yoshino H, Kubo S, Sato K, Hattori T, Lu CS, Inzelberg R, Djaldetti R, Melamed E, Amouri R, Gouider-Khouja N, Hentati F, Hatano Y, Wang M, Imamichi Y, Mizoguchi K, Miyajima H, Obata F, Toda T, Farrer MJ, Mizuno Y, Hattori N (2006) Clinicogenetic study of mutations in *LRRK2* exon 41 in Parkinson's disease patients from 18 countries. Mov Disord 21:1102–1108

Wu T, Zeng Y, Ding X, Li X, Li W, Dong H, Chen S, Zhang X, Ma G, Yao J, Deng X (2006) A novel P755L mutation in LRRK2 gene associated with Parkinson's disease. NeuroReport 17:1859–1862

Zimprich A, Biskup S, Leitner P, Lichtner P, Farrer M, Lincoln S, Kachergus J, Hulihan M, Uitti RJ, Calne DB, Stoessl AJ, Pfeiffer RF, Patenge N, Carbajal IC, Vieregge P, Asmus F, Müller-Myhsok B, Dickson DW, Meitinger T, Strom TM, Wszolek ZK, Gasser T (2004) Mutations in LRRK2 cause autosomal-dominant parkinsonism with pleomorphic pathology. Neuron 44:601–607

STEM CELLS
TISSUE-SPECIFIC STEM CELLS

Molecular Signature of Quiescent Satellite Cells in Adult Skeletal Muscle

SO-ICHIRO FUKADA,[a] AKIYOSHI UEZUMI,[a] MADOKA IKEMOTO,[a] SATORU MASUDA,[a] MASASHI SEGAWA,[b] NAOKI TANIMURA,[c] HIROSHI YAMAMOTO,[b] YUKO MIYAGOE-SUZUKI,[a] SHIN'ICHI TAKEDA[a]

[a]Department of Molecular Therapy, National Institute of Neuroscience, National Center of Neurology and Psychiatry, Tokyo, Japan; [b]Department of Immunology, Graduate School of Pharmaceutical Sciences, Osaka University, Osaka, Japan; [c]Bio and Nano Technologies, Science and Technology Division, Mizuho Information & Research Institute Inc., Tokyo, Japan

Key Words. Fluorescence-activated cell sorting • Microarray • Quiescence • Muscle satellite cells • Calcitonin receptor

ABSTRACT

Skeletal muscle satellite cells play key roles in postnatal muscle growth and regeneration. To study molecular regulation of satellite cells, we directly prepared satellite cells from 8- to 12-week-old C57BL/6 mice and performed genome-wide gene expression analysis. Compared with activated/cycling satellite cells, 507 genes were highly upregulated in quiescent satellite cells. These included negative regulators of cell cycle and myogenic inhibitors. Gene set enrichment analysis revealed that quiescent satellite cells preferentially express the genes involved in cell-cell adhesion, regulation of cell growth, formation of extracellular matrix, copper and iron homeostasis, and lipid transportation. Furthermore, reverse transcription-polymerase chain reaction on differentially expressed genes confirmed that calcitonin receptor (CTR) was exclusively expressed in dormant satellite cells but not in activated satellite cells. In addition, CTR mRNA is hardly detected in nonmyogenic cells. Therefore, we next examined the expression of CTR in vivo. CTR was specifically expressed on quiescent satellite cells, but the expression was not found on activated/proliferating satellite cells during muscle regeneration. CTR-positive cells reappeared at the rim of regenerating myofibers in later stages of muscle regeneration. Calcitonin stimulation delayed the activation of quiescent satellite cells. Our data provide roles of CTR in quiescent satellite cells and a solid scaffold to further dissect molecular regulation of satellite cells. STEM CELLS *2007;25:2448–2459*

Disclosure of potential conflicts of interest is found at the end of this article.

INTRODUCTION

Muscle satellite cells, which account for 2%–5% of the total nuclei in adult skeletal muscle, play a major role in muscle regeneration [1, 2]. Under normal conditions, satellite cells are found external to the myofiber plasma membrane and beneath the muscle basal lamina [3] and are mitotically quiescent in the adult skeletal muscle [4, 5]. When activated by muscle damage, they proliferate, differentiate, fuse with each other or injured fibers, and eventually regenerate mature myofibers under the influence of innervation [6]. Recently, it was clearly demonstrated that the proliferation capacity of satellite cells in vivo is robust and that the contribution of interstitial cells or bone marrow-derived cells to muscle fiber regeneration is limited [7]. Importantly, a small fraction of activated satellite cells exit the cell cycle and return to the quiescent satellite state during muscle regeneration to maintain their numbers and the regenerative capacity of muscle.

Besides muscle fiber repair, satellite cells are also responsible for postnatal growth [8] and hypertrophy of skeletal muscle [9], and impairment of their functions is related to several pathological conditions, for example, muscular dystrophies and aging-related muscle atrophy [10]. Moreover, several studies showed that satellite cells differentiate into adipogenic cells or osteocytes in vitro [11–13], implying that they contribute to the fatty infiltration seen in Duchenne muscular dystrophy. Thus, normal functioning of satellite cells is indispensable for the integrity of skeletal muscle, and the cells themselves are an important source of cells for cell therapy of muscle diseases, making it valuable to clarify the molecular regulation of maintenance, activation/proliferation, and differentiation in satellite cells.

Like hematopoietic stem cells, most satellite cells are in a quiescent and undifferentiated state in the adult. Although quiescence is important to retain the proliferative and differentiative potential of satellite cells throughout the lifetime, the molecular regulation of quiescence remains poorly defined. Recent studies suggested that myostatin, a skeletal muscle-specific transforming growth factor-β superfamily member, suppresses the activation of satellite cells [14]. Myostatin has been shown to induce a potent cyclin-dependent kinase inhibitor, p21(Cdkn1a), in vitro [15]. Other in vitro studies suggested that the decrease of MyoD protein and induction of another cyclin-dependent kinase inhibitor, p27(Cdkn1b) [16], and a Rb-related pocket protein, p130 [16, 17], are involved in the attainment of quiescence by proliferating myoblasts.

Correspondence: Yuko Miyagoe-Suzuki, M.D., Ph.D., Department of Molecular Therapy, National Institute of Neuroscience, National Center of Neurology and Psychiatry, 4-1-1 Ogawa-higashi, Kodaira, Tokyo 187-8502, Japan. Telephone: +81-42-346-1720; Fax: +81-42-346-1750; e-mail: miyagoe@ncnp.go.jp Received January 8, 2007; accepted for publication June 19, 2007; first published online in STEM CELLS *EXPRESS* June 28, 2007. 1066-5099/2007/$30.00/0 doi: 10.1634/stemcells.2007-0019

We previously reported a method to purify quiescent satellite cells from adult skeletal muscle using the fluorescence-activated cell sorting (FACS) technique and a novel antibody named SM/C-2.6 [18]. In this study, to clarify the molecular regulation of quiescent satellite cells, we performed genome-wide gene expression profiling of quiescent satellite cells isolated from C57BL/6 mice. Expression analysis of individual genes identified several candidate genes that regulate dormancy of satellite cells. Gene set enrichment analysis (GSEA) revealed that the gene sets involved in cell-cell adhesion, cell growth, copper and iron ion homeostasis, lipid transport, and formation of extracellular matrix were coordinately upregulated in quiescent satellite cells. Furthermore, we demonstrate that calcitonin receptor (CTR) is expressed specifically on quiescent satellite cells in vivo and that calcitonin significantly attenuates the activation of satellite cells. Our study is the first report of in-depth gene expression analysis of quiescent satellite cells and will greatly facilitate the investigation of molecular regulation of satellite cells in both physiological and pathological conditions.

MATERIALS AND METHODS

Animals

All procedures using experimental animals were approved by the Experimental Animal Care and Use Committee at the National Institute of Neuroscience. C57BL/6 mice were purchased from Nihon CLEA (Tokyo, http://www.clea-japan.com).

Preparation of Satellite Cells and Nonmyogenic Cells from Mouse Limb Muscles

Mononuclear cells were prepared from fore- and hindlimb muscles of 8- to 12-week-old female C57BL/6 mice as described [19] and incubated on ice for 30 minutes in the presence of a 1:200 dilution of phycoerythrin-conjugated anti-CD45 (clone: 30-F11) and biotinylated SM/C-2.6 [18]. Cells were then incubated with streptavidin-labeled allophycocyanin on ice for 30 minutes and resuspended in phosphate-buffered saline (PBS) containing 2% fetal bovine serum (FBS) and 2 μg/ml propidium iodide (PI). Cell sorting was performed on a FACSVantage SE flow cytometer (BD Biosciences, San Diego, http://www.bdbiosciences.com). Dead cells were excluded by PI gating. All antibodies and reagents for FACS analysis were purchased from BD Pharmingen (San Diego, http://www.bdbiosciences.com/index_us.shtml).

Cell Culture

Satellite cells were cultured in growth medium consisting of high-glucose Dulbecco's modified Eagle's medium (DMEM; Invitrogen, Carlsbad, CA, http://www.invitrogen.com) containing 20% fetal calf serum (FCS; Trace Biosciences, New South Wales, Australia), 2.5 ng/ml basic fibroblast growth factor (Invitrogen), and penicillin (100 U/ml)-streptomycin (100 μg/ml) (Gibco-BRL, Gaithersburg, MD, http://www.gibcobrl.com) on culture dishes coated with Matrigel (BD Biosciences). Single living myofibers were prepared as described [20] and transferred to Matrigel-coated 24-well culture dishes (one fiber per well). After a 2-day culture in growth medium with or without elcatonin, satellite cells that had detached from muscle fibers were counted.

Immunocytochemical Analysis

FACS-sorted cells were collected on glass slides by Cytospin 3 (Thermo Shandon Inc., Pittsburgh, http://www.thermo.com) and immunostained as described [19]. Cultured cells were fixed on 8-well Lab-Tek Chamber Slides (Nunc, Rochester, NY, http://www.nuncbrand.com) and stained as described [19, 21] with mouse anti-Pax7 (1:100; clone: Pax7; Developmental Studies Hybridoma Bank, Iowa City, IA, http://www.uiowa.edu/~dshbwww), mouse anti-MyoD (1:200; clone: 5.8A; NeoMarkers; Lab Vision, Fremont, CA, http://www.labvision.com), mouse anti-myogenin (1:100; clone: F5D; Developmental Studies Hybridoma Bank), rabbit anti-Ki67 (1:2; Ylem, Rome), or rabbit anti-p57 antibodies (1:50; GeneTex, San Antonio, http://www.genetex.com) at 4°C overnight and then reacted with secondary antibodies conjugated with Alexa 488 or Alexa 568 (Molecular Probes, Eugene, OR, http://probes.invitrogen.com). Nuclei were stained with 4,6-diamidino-2-phenylindole (DAPI). Images were photographed using a phase-contrast and fluorescence microscope IX70 (Olympus, Tokyo, http://www.olympus-global.com) equipped with a Quantix air-cooled CCD camera (Photometrics, Kew, VIC, Australia, http://www.photometrix.com.au) and IP Lab software (Scanalytics, Rockville, MD, http://www.scanalytics.com).

Immunohistochemistry

Immunostaining of muscle cryosections was performed as previously described [21] using rat anti-laminin α2 (1:200; clone 4H8-2; Alexis Biochemical, Lausen, Switzerland, http://www.axxora.com), rabbit anti-M-cadherin [21], rabbit anti-human CTR (1:200; Serotec Ltd., Oxford, U.K., http://www.serotec.com), goat anti-Notch 3 (1:100; R&D Systems Inc., Minneapolis, http://www.rndsystems.com), or mouse anti-Pax7. Rabbit anti-mouse HeyL polyclonal antibody was produced in our laboratory. In brief, the DNA fragment corresponding to amino acids 220–287 of mouse HeyL (GenBank: NM_013905) was fused to glutathione *S*-transferase in the pGEX-1 Lambda T vector (GE Healthcare, Uppsala, Sweden, http://www.gehealthcare.com). The purified fusion protein was used to immunize New Zealand White rabbits. The obtained serum was affinity-purified. For Pax7 staining, an M.O.M. kit (Vector Laboratories, Burlingame, CA, http://www.vectorlabs.com) was used to block endogenous mouse IgG. For CTR staining, horseradish peroxidase-conjugated anti-rabbit IgG donkey secondary antibody (1:100; GE Healthcare) and Alexa 568-conjugated Tyramid (Molecular Probes) were used to amplify the signal. Nuclei were counterstained with TOTO-3 (1:5,000; Molecular Probes) or DAPI. The images were recorded using a confocal laser scanning microscope system TCSSP (Leica, Heerbrugg, Switzerland, http://www.leica.com) or Axiophot microscope (Carl Zeiss, Jena, Germany, http://www.zeiss.com).

Cell Cycle Analysis

Muscle-derived mononucleated cells or cultured SM/C-2.6 positive cells were suspended at 10^6 cells per milliliter in DMEM (Invitrogen) containing 2% FBS (Trace Biosciences), 10 mM Hepes, and 10 μM Hoechst 33342 (Sigma-Aldrich, St. Louis, http://www.sigmaaldrich.com) and incubated for 45 minutes at 37°C. An additional incubation was performed in the presence of 10 μg/ml Pyronin Y (Sigma-Aldrich) for 45 minutes at 37°C. Cells were then washed with PBS containing 2% FCS. Muscle-derived mononucleated cells were stained with SM/C-2.6 antibody and analyzed by FACSVantage SE flow cytometer.

Cell Proliferation Assay

After cell sorting, quiescent satellite cells were plated on 96-well culture plates at a density of 3,000–8,000 in the absence or presence of elcatonin (0.01–0.1 U/ml) (Asahi Kasei Pharma Corporation, Tokyo, http://www.asahi-kasei.co.jp/asahi/en) and cultured for 1–2 days. Then 5-bromo-2′-deoxyuridine (BrdU) (10 μM) was added to the culture. To examine the effects of elcatonin on activated satellite cells, satellite cells were cultured for 3 days and then elcatonin was added to the culture 24 hours before addition of BrdU. Twenty-four hours later, BrdU uptake was quantified by cell proliferation enzyme-linked immunosorbent assay, BrdU Kit (Roche Diagnostics, Basel, Switzerland, http://www.roche-applied-science.com), and lumi-Image F1 (Roche). In Figure 6B, cells were exposed to elcatonin for 30 minutes and washed twice with PBS and then plated on culture dishes.

Detection of Apoptotic Cells

Cells were cultured on 8-well Lab-Tek chamber slides with or without elcatonin. Apoptotic cells were detected by rhodamine fluorescence using an ApopTag Red In Situ Apoptosis Detection Kit (Chemicon, Temecula, CA, http://www.chemicon.com).

RNA Extraction and Reverse Transcription-Polymerase Chain Reaction

Total RNA was extracted from sorted or cultured cells with a Qiagen RNeasy Mini kit according to the manufacturer's instructions (Qiagen, Hilden, Germany, http://www1.qiagen.com) and then reverse-transcribed into cDNA by using TaqMan Reverse Transcription Reagents (Roche). The polymerase chain reaction (PCR) was performed with cDNA products under the following cycling conditions: 94°C for 3 minutes followed by 30–40 cycles of amplification, annealing, and extension (94°C for 15 seconds, 58°C for 30 seconds, and 72°C for 30 seconds) with a final incubation at 72°C for 5 minutes. Specific primer sequences used for PCR are described in supplemental online Materials and Methods.

Target Synthesis, Gene Chip Hybridization, and Data Acquisition

To label antisense RNA (aRNA) with biotin for microarray hybridization, we followed the protocol supplied by the manufacturer (Affymetrix, Santa Clara, CA, http://www.affymetrix.com). Because the starting amount of total RNA was 100 ng for the sorted SM/C-2.6$^+$ cell fraction, we used a two-cycle biotin aRNA synthesis kit (Affymetrix). Labeled aRNA was fragmented according to Affymetrix GeneChip protocol and then hybridized to Affymetrix MOE430A GeneChip arrays for 16 hours. After washing, the gene chips were stained according to the instrument's standard Eukaryotic GE WS2v4 protocol using antibody-mediated signal amplification. The signal was determined, using the Microarray Suite (MAS) 5.0 absolute analysis algorithm, as the average fluorescence intensity among the intensities obtained from the probe set. The signal of a probe set was calculated as the one-step biweight estimate of combined differences of all the probe pairs (perfectly matched and mismatched) in the probe set. A one-sided Wilcoxon's signed rank test was used to calculate a p value that reflects the significance of differences between perfectly matched and mismatched probe pairs. The p value was used to make the absolute call for probe sets. A "Present" call was assigned to transcripts for p values between 0 and .04, a "Marginal" call was assigned to transcripts for p values between .04 and .06, and an "Absent" call was assigned to transcripts for p values between .06 and 1.0.

Microarray Data Analysis

Scanned output files were analyzed by the probe level analysis package MAS 5.0 (Affymetrix). The Present/Absent call provided by the Affymetrix programs was used for the first selection. The MAS 5.0-generated raw data were uploaded to GeneSpring software version 7.0 (Silicongenetics, Redwood, CA, http://www.chem.agilent.com/scripts/PHome.asp). Data normalization was achieved by one of two methods: (a) each signal was divided by the 50th percentile of all signals in a specific hybridization experiment or (b) each signal was divided by the median of its values in all samples. A more reliable list of "5-fold changing" genes was obtained by applying the filtering options of GeneSpring. Present calls in all (four) quiescent or activated satellite cell probes were selected and a restriction, which passed genes with raw data above 100, was applied. Then, using all the quiescent and activated satellite cells as data, we performed a one-way analysis of variance test between the quiescent satellite cell group and the activated satellite cell group. In particular, a parametric test, with variances assumed equal (Student's t test, p value cut-off .05; multiple testing correction: Benjamini and Hochberg false discovery rate), was applied. The genes passing all these filters and tests were selected as "5-fold changing genes." Nonmyogenic cells (SM/C-2.6$^-$/CD45$^-$ cells) were also prepared four times.

Gene Set Enrichment Analysis

GSEA [22] is a statistical analysis of sets of gene expression profiles, separated by phenotypic labels. Using GSEA, we can test hypotheses concerned with predefined sets of genes; the rank orderings of the genes in the whole gene set calculated with a given ranking method are random with regard to a given classification of samples. As a result of the analysis, nominal p values, family-wise error rate p values, and false discovery rate (FDR) q values for test hypotheses (thus for gene sets) were obtained.

In our analysis, we used the GSEA-P software package [22], which is available from the Broad Institute (Cambridge, MA, http://www.broad.mit.edu). We prepared, as input to the GSEA-P, the MAS 5.0-generated raw signal data and gene sets derived independently. We chose genes on the chip that were detected (the Present call was assigned) in at least one sample (17,150 of 22,626). The raw signals of the chosen genes were normalized so that their total sum was 1. Because the total amount of mRNA in a quiescent satellite cell (QSC) is much less than that in an activated satellite cell (ASC), the normalized signal should be understood as a relative signal among the chosen genes. To compile the gene sets, we assigned each probe to a gene ontology (GO) category [23] using annotations of the MOE430A chip (September 22, 2005) provided by Affymetrix. Therefore, these gene sets reflect the structure of the GO categories and subcategories of molecular function (MF), biological process (BP), and cellular component (CC). The 17,150 genes chosen comprised 1,674, 1,698, and 412 gene sets in the MF, BP, and CC subcategories, respectively, and were reduced to 162, 218, and 85 after filtering out gene sets with sizes smaller than 20 or larger than 1,000. We ran the GSEA-P with the signal-to-noise option for its ranking metric, with permutation over phenotype labels of QSC and ASC samples, and repeated it 2,000 times with the "weighted" option for its scoring scheme.

Results and Discussion

Isolation of Quiescent Satellite Cells from Mouse Skeletal Muscle

First, to obtain RNA samples for microarray analysis, we prepared mononuclear cells from 8- to 12-week-old C57BL/6 mouse muscle, and the SM/C-2.6$^+$ fraction was collected as the satellite cell fraction by FACS [18] (Fig. 1A). Consistent with our previous report, more than 97% of fresh SM/C-2.6$^+$ cells expressed Pax7 (Fig. 1B) but were mostly negative for both MyoD (Fig. 1Ca, 1Cb) and Ki67 (Fig. 1Ce, 1Cf). After 4–5 days of culture, more than 98% of SM/C-2.6$^+$ cells expressed MyoD (Fig. 1Cg, 1Ch) and Ki67 (Fig. 1Ck, 1Cl). Both freshly isolated, uncultured SM/C-2.6$^+$ cells and SM/C-2.6$^+$ cells cultured in growth medium were negative for myogenin expression (Fig. 1Cc, 1Cd, 1Ci, 1Cj), but these cells started to express myogenin and differentiated well into multinucleated myotubes after mitogen withdrawal (data not shown). In contrast, more than 99% of freshly isolated SM/C-2.6$^-$/CD45$^-$ cells were negative for Pax7 expression (Fig. 1Bc, 1Bd), and cultured SM/C-2.6$^-$/CD45$^-$ cells did not express MyoD (data not shown), again indicating that myogenic cells are highly enriched in the SM/C-2.6$^+$ fraction.

The forward and side scatter profiles of freshly isolated SM/C-2.6$^+$ cells showed that they are small and uniform in granularity (data not shown). In fact, as shown in Figure 1D, the cell size of fresh SM/C-2.6$^+$ cells was estimated to be approximately one-half that of cultured SM/C-2.6$^+$ cells based on the forward scatter profile, indicating that the freshly isolated SM/C-2.6$^+$ cells were not activated yet. Pyronin Y staining showed the small amount of RNA content in freshly isolated SM/C-2.6$^+$ cells (Fig. 1D). In general, a Pyronin^{low} and Hoechst 33342^{low} fraction is considered

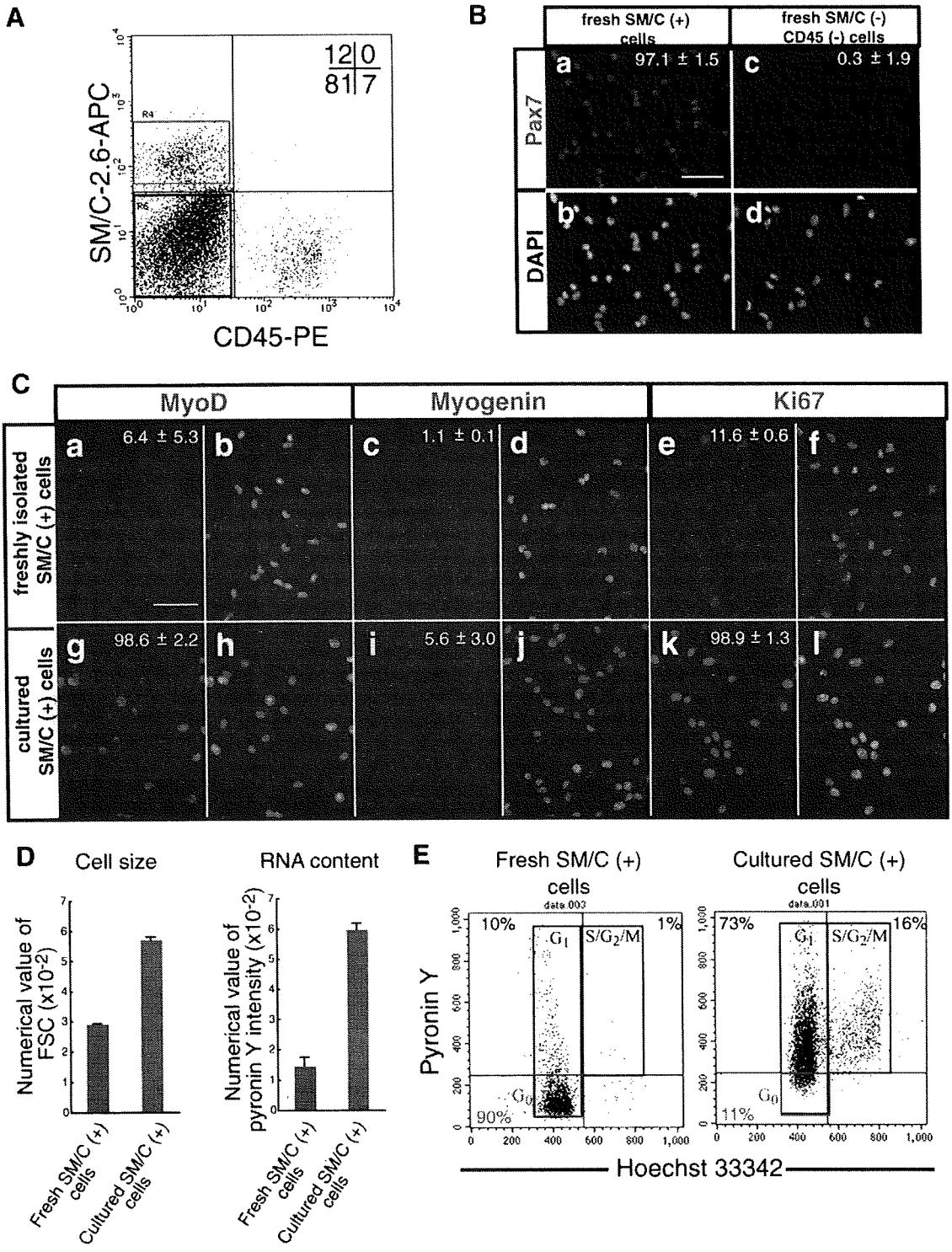

Figure 1. SM/C-2.6$^+$ cells isolated from skeletal muscle by fluorescence-activated cell sorting (FACS) are highly purified quiescent satellite cells and proliferate and express MyoD in culture. **(A):** Mononucleated cells prepared from uninjured limb muscles of adult mice were stained with anti-CD45 antibody and SM/C-2.6 monoclonal antibody. The SM/C-2.6$^+$ fraction (red square) and the SM/C-2.6$^-$/CD45$^-$ fraction (blue square) were collected for further analysis. **(B):** Freshly isolated SM/C-2.6$^+$ and SM/C-2.6$^-$/CD45$^-$ cells were stained with anti-Pax7 **(Ba, Bc)** antibody and DAPI **(Bb, Bd)**. The percentages of Pax7-positive cells in each cell fraction are shown. Cell fractionation was performed three times, and more than 300 cells from each fraction were counted. Scale bar: 50 μm. **(C):** Freshly isolated SM/C-2.6$^+$ cells and SM/C-2.6$^+$ cells cultured for 4 days in the presence of basic fibroblast growth factor were stained with antibodies to MyoD **(Ca, Cg)**, myogenin **(Cc, Ci)**, or Ki67 **(Ce, Ck)**. Percentages of MyoD-, myogenin-, or Ki67-positive cells are shown. Cell fractionation was performed three times, and more than 180 cells were counted each time. Nuclei were stained with DAPI **(Cb, Cd, Cf, Ch, Cj, Cl)**. Scale bar: 50 μm. **(D):** The mean value of FSC (cell size) and Pyronin Y intensity (RNA content) of freshly isolated SM/C-2.6$^+$ cells and satellite cells cultured in vitro. The value is an average of two independent experiments. **(E):** The percentages of cells in the G0 phase of the cell cycle were estimated by staining with Pyronin Y and Hoechst 33342. The number in the lower left of each FACS profile indicates the percentage of the G0 cells: 90% for fresh SM/C-2.6$^+$ cells and 11% for cultured SM/C-2.6$^+$ cells. Abbreviations: APC, allophycocyanin; DAPI, 4,6-diamidino-2-phenylindole; FSC, forward scatter; M, mitosis phase; PE, phycoerythrin; S, synthesis phase.